

## Research Article

# Optimization on Wear Rate of AA2219/Nanographite/TiB<sub>2</sub>/Si<sub>3</sub>N<sub>4</sub> Hybrid Composites Using Taguchi Process

A. Chandra Shekar,<sup>1</sup> Gurusamy Pathinettampadian,<sup>2</sup> R. Suthan,<sup>3</sup> Melvin Victor De Poures,<sup>4</sup> Sultan Althahban,<sup>5</sup> S. Mousa,<sup>6</sup> Faez Qahtani,<sup>7</sup> Yosef Jazaa,<sup>8</sup> and Belachew Girma <sup>9</sup>

<sup>1</sup>Department of Mechanical Engineering, Bangalore Institute of Technology, Bengaluru, India

<sup>2</sup>Department of Mechanical Engineering, Chennai Institute of Technology, Chennai, India

<sup>3</sup>Department of Mechanical Engineering, Panimalar Engineering College, Chennai, India

<sup>4</sup>Department of Thermal Engineering, Saveetha School of Engineering, SIMATS, Chennai, Tamil Nadu, India

<sup>5</sup>Department of Mechanical Engineering, Jazan University, Jazan 82822, Saudi Arabia

<sup>6</sup>Faculty of Engineering, Jazan University, Jazan 706, Saudi Arabia

<sup>7</sup>Department of Mechanical Engineering, Najran University, Najran, 11001, Saudi Arabia

<sup>8</sup>Faculty of Engineering, King Khalid University, Saudi Arabia

<sup>9</sup>Department of Mechanical Engineering, Mizan Tepi University, Ethiopia

Correspondence should be addressed to Belachew Girma; belachewgt@mtu.edu.et

Received 17 March 2022; Accepted 17 June 2022; Published 9 July 2022

Academic Editor: Palanivel Velmurugan

Copyright © 2022 A. Chandra Shekar et al. This is an open access article distributed under the Creative Commons Attribution License, which permits unrestricted use, distribution, and reproduction in any medium, provided the original work is properly cited.

The various following reinforcements like nanographite, titanium diboride (TiB<sub>2</sub>), silicon nitride (Si<sub>3</sub>N<sub>4</sub>), and aluminum 2219 have all been investigated in this study. Current research suggests that TiB<sub>2</sub> and graphite may be a suitable reinforcement for Al2219 alloy. The stir casting process was used to make reinforced composites on unreinforced Al2219. Compared to the unreinforced Al2219, the TiB<sub>2</sub> and nanographite-reinforced hybrid composites showed the exceptional wear resistance (30%) at 175°C. Matrix strengthening kinetics is improved at 175°C when TiB<sub>2</sub> and nano-Gr reinforcement particles are present. To obtain a *p* value less than 1% and an absolute relative error of less than 1%, an artificial neural network was employed.

## 1. Introduction

As a result of technological advancements, we now have access to higher-quality goods and services [1]. A design taken into account the practical need and its production aspects can improve the quality of goods. The synthesis technique should be carefully considered as part of the design process in order to produce the best possible product at the lowest possible cost [2, 3]. Furthermore, in today's modern industries, a productive manufacturing process is a must-have. Additionally, the product must be reasonably priced and functional in terms of both the environment and its aesthetic appeal, as well [4]. As a result of their high

ratios of strength to mass, aluminum alloys are critical to the transportation industry. Despite this, adhesion is a common problem when working with these alloys [5–7]. AMMCs (aluminum metal matrix composites) are better than aluminum alloys at replacing them because of their properties. Compared to monolithic materials, AMMCs are more resistant to wear [8]. In the aerospace, aircraft, and automobile industries, ceramic-reinforced composites are advancing rapidly. These materials have superior mechanical and physical properties because of their lower specific gravity [9, 10].

Studying the reinforcing ceramics in composite materials aims to learn more about the materials' composition,

structural characteristics, and physical properties [11]. The material's constituent phases must be altered in order to improve its properties. Stiffness, creep, and wear resistance were all significantly improved by adding small amounts of hard, strong particles. Ceramic reinforcement dispersion in AMMCs has long been recognized as a significant contributor to AMMCs' increased rigidity and wear resistance [12–14]. The adding of graphite or silicon carbide to Al-Gr/Al-SiC composite was not favorable above a certain point. Wear resistance can be improved by using graphite as a main compliance and silicon as subordinate compliance, which create a shielding layer between composite pin and counterpart [15].  $\text{Si}_3\text{N}_4$ -reinforced Al alloys have a higher hardness. SiC,  $\text{Al}_2\text{O}_3$ , and  $\text{TiB}_2$  have all been used as refinement materials in a number of research projects. The  $\text{TiB}_2$  particles, on the other hand, have a limited application [16]. Alloying silicon was a well-known component of utmost aluminum casting alloys (Si). The three important types of aluminum-silicon alloys are hypereutectic (14-25 weight % of silicon), eutectic (12-13 weight % of silicon), and hypoeutectic (12 weight % of silicon) [17]. Copper and magnesium were added to Al alloys in order to increase the efficiency of the engine block, which works at a wide range of temperatures and stresses. Aluminum alloy's strength and hardness are affected at room temperature and higher by copper (Cu, 0.2-2.5 w.t. percent) [18–20].

## 2. Experimental Procedure

Researchers in the field of metallurgy found the artificial neural network (ANN) to be the most effective algorithm. Many technical and scientific problems can be solved using this statistical method. As far as advancements in 2219 aluminum alloys reinforced with titanium diboride-nanographite,  $\text{Si}_3\text{N}_4$ -nanographite particles, as in Table 1 and dry sliding wear properties at maximum temperature, are concerned, and the literature provides little information. The current research was focused on developing new hybrid composites in accordance with the literature review. Consequently, this study is aimed at examining maximum temperature of dry sliding wear characteristics of AA 2219 (Al, 0.02 percent Mg, 0.2% Si, 6.8% Cu, 0.2 percent Zr) with ceramic particles  $\text{Si}_3\text{N}_4$ ,  $\text{TiB}_2$ , and nanographite. Stir casting was used to create new AMMCs as in Figure 1.

Table 2 lists the chemical components of Al 2219. To avoid casting defects, a layer of slag was added to the crucible as the ingots melted and turned liquid. After that, commercially available weighed and preheated  $\text{TiB}_2$  and  $\text{Si}_3\text{N}_4$  (30 microns) were added to the crucible as a reinforcement. It is necessary to use a crucible to achieve a properly homogeneous mixture to achieve the desired stirring times (150 rpm). An additional reinforcement of preheated nanographite particles (40 nm) was added to the furnace as in Table 3, and the similar process was used to attain a regular mixture [21]. Slurry of liquefied metal is transferred into a split type heated graphite mould. Reinforcement weight percent of  $\text{Si}_3\text{N}_4$ , nanographite, and  $\text{TiB}_2$  powder was used to synthesize the hybrid composites.

TABLE 1: Materials used for the synthesis of composite.

| Materials used for the synthesis of composite         |
|---|
| Aluminum 2219   |
| Magnesium as a wettability agent                      |
| Titanium diboride ( $\text{TiB}_2$ )                  |
| Nanographite particles                                |
| Silicon nitride ( $\text{Si}_3\text{N}_4$ )           |
| Hexa-chloroethane to remove gas from the molten metal |

**2.1. Hardness Test.** Chromium steel or tungsten carbide was used to test a specimen's hardness by pressing it against the surface. In accordance with ASTM E-10 standards, samples were prepared. At 240 kgf and a dwell time of 30 seconds, digital testers reported the hardness number.

**2.2. Wear Test.** It is useful to conduct wear tests in order to determine the product's wear characteristics. The measuring method determines whether or not wear is measurable. Wear rate can be measured in two ways, namely, mass and volume loss, where the mass-loss method is the most applicable one. This technique of weight loss should not affect by condensed humidity and further external contaminants, like as oil and dust [22]. It is possible to measure wear by volume loss, but this method is more sensitive. Dry sliding wear behavior of Al2219 and AMMCs was studied by pin-on-disc testing device. According to G99 standard, the AMMC's pins were developed to slide in contradiction of a revolving steel disc (EN-32) at various temperatures, such as 75°C, 125°C, and 175°C. The specimen and disc were cleaned with acetone during the experiment. Protecting the test pin and steel disc from exposure to the environment is acetone's primary function. It was measured with an electronic balance weigher both before and after the experiment (0.0001 g resolution).

**2.3. Design of Experiments.** The experiments are designed using Taguchi's orthogonal array L27. The input parameters are the load, speed, distance, and temperature, as in Table 4 while the response parameter is the wear rate. Table 5 summarizes the experimental design, as well as the mean values of the various variables [23].

## 3. Result and Discussions

**3.1. Hardness Test.** The hardness values of the test samples are shown in Figure 2. Sample A2 has been confirmed to have a harder surface than samples A1 and A. The hardness of the composites was increased by the presence of  $\text{TiB}_2$  and graphite. The composite's hardness is influenced by the strengthening effect of nanographite as well as the hardness of  $\text{TiB}_2$ , which was the composite's third hardest material.

**3.2. Wear Analysis at Different Temperatures.** The oxide shifted coating forms and protects the worn surface. By reducing the number of metal-to-metal links at the edge, it is able to lose less weight. At higher loads, the tribolayer ruptures and increases wear as in Figure 3, despite the fact that it is not a permanent layer [24]. The new Al-Cu-Mg alloy and

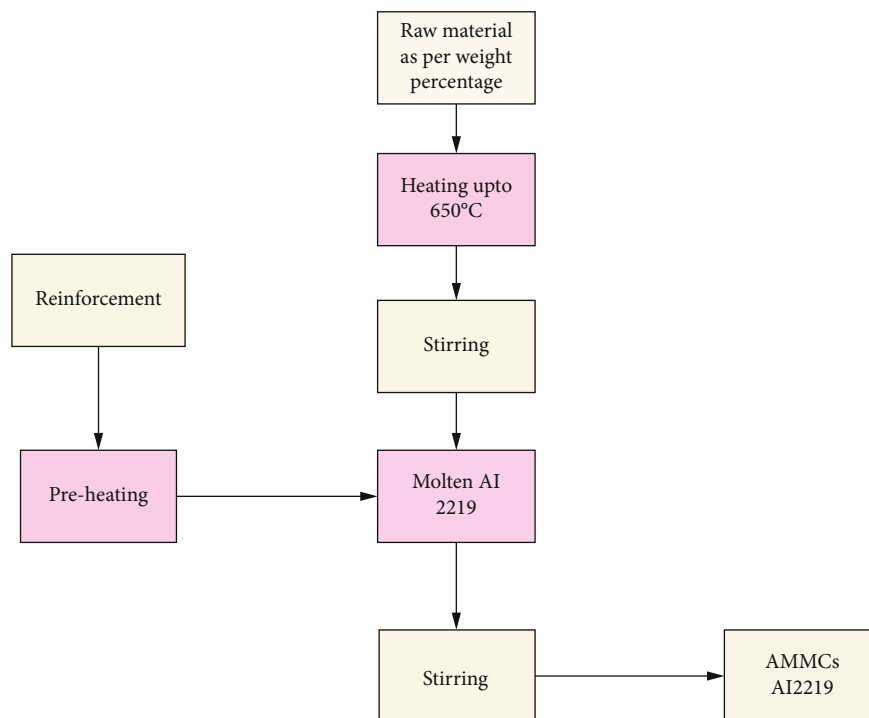


FIGURE 1: Methodology adopted for AMMC casting.

TABLE 2: The 2219 Aluminum alloy's components.

| Constituents | Silicon | Magnesium | Zirconium   | Copper      | Iron | Manganese | Titanium | Vernadium | Zinc  |
|--------------|---------|-----------|-------------|-------------|------|-----------|----------|-----------|-------|
| % of weight  | 0.20    | 0.02      | 0.10 – 0.24 | 5.70 – 6.80 | 0.30 | 0.020     | 0.020    | 0.050     | 0.100 |

TABLE 3: Percentage of material composition.

| Sample | Al 2219 | TiB <sub>2</sub> wt. % | Si <sub>3</sub> N <sub>4</sub> wt. % | Nanographite wt. % |
|--------|---------|------------------------|--------------------------------------|--------------------|
| A      | 100     | –                      | –                                    | –                  |
| A1     | 90      | –                      | 5                                    | 5                  |
| A2     | 90      | 5                      | –                                    | 5                  |

TABLE 4: Factors and their levels used in the study.

| Factors                  | Levels |     |     |
|--------------------------|--------|-----|-----|
|                          | 1      | 2   | 3   |
| Load (Newton)            | 25     | 35  | 45  |
| Speed (meter/sec)        | 1.5    | 3   | 4.5 |
| Sliding distance (meter) | 500    | 625 | 750 |
| Temperature (°C)         | 75     | 125 | 175 |

matrix phase had an incoherent interface. This has an effect on wear rate. Temperature caused the Al2219 alloy surface to wear more quickly than the Si<sub>3</sub>N<sub>4</sub> reinforced composite. Si<sub>3</sub>N<sub>4</sub> and matrix work together to create a wear-resistant alloy that is superior to unreinforced alloy. There has been no conversion between slight and severe wear in terms of temperature.

Wear resistance of composite (A1) decreased at 175°C, which is consistent with the results. The normal load was varied throughout the tests. A material's surface can never be perfectly flat at the atomic level. Surfaces come into contact with each other at various points when they are in contact. Plastic deformation occurs at those points when the load is applied, resulting in the removal of material. The greater the load, the greater the amount of plastic deformation will be [25]. As a result, at 35 N, the wear rate will be higher. The rate of plastic deformation is dependent on the applied load; so, the wear rate is lower at 25 N. In contrast, one of the most common mechanisms for causing wear is delamination. While sliding against each other under load and heat, wear particles can be seen to separate into sheets or flakes. Taking plastic deformation and flow into account at the asperities is another benefit of the ploughing action. Nanographite serves as a secondary reinforcement. It has excellent lubricating properties due to its unusual molecular structure, which includes a hexagonal carbon piece held together by robust hybridized carbon-carbon connection [26]. Equiaxed crystals were formed primarily as an outcome of uniform chilling process. The rate of heat dissipation was reasonable because of the effect of TiB<sub>2</sub> and nanographite, and as result, even crystals were developed.

Reinforcement was able to maintain the wear resistance of the AMMC even though the temperature reached 175°C.

TABLE 5: Layout plan and experimental results.

| x  | Load (Newton) | Speed (meter/sec) | Distance (meter) | Temperature ( $^{\circ}$ C) | Wear rate mm/m <sup>3</sup> |           |          |
|----|---------------|-------------------|------------------|-----------------------------|-----------------------------|-----------|----------|
|    |               |                   |                  |                             | Sample A2                   | Sample A1 | Sample A |
| 1  | 25            | 1.5               | 500              | 75                          | 0.9358                      | 1.1471    | 1.2734   |
| 2  | 25            | 1.5               | 625              | 125                         | 0.5924                      | 0.6537    | 0.7456   |
| 3  | 25            | 1.5               | 750              | 175                         | 0.2907                      | 0.3854    | 0.5376   |
| 4  | 25            | 3                 | 500              | 125                         | 1.1898                      | 1.4456    | 1.3045   |
| 5  | 25            | 3                 | 625              | 175                         | 0.9567                      | 1.1567    | 1.2435   |
| 6  | 25            | 3                 | 750              | 75                          | 1.2063                      | 1.3560    | 1.4436   |
| 7  | 25            | 4.5               | 500              | 175                         | 0.9547                      | 1.1497    | 1.3876   |
| 8  | 25            | 4.5               | 625              | 125                         | 1.243                       | 1.5945    | 1.5578   |
| 9  | 25            | 4.5               | 750              | 75                          | 1.1493                      | 1.2775    | 1.4956   |
| 10 | 35            | 1.5               | 500              | 75                          | 1.1127                      | 1.2731    | 1.1674   |
| 11 | 35            | 1.5               | 625              | 125                         | 0.7908                      | 0.9685    | 1.0445   |
| 12 | 35            | 1.5               | 750              | 175                         | 1.0401                      | 1.1413    | 1.2876   |
| 13 | 35            | 3                 | 500              | 125                         | 1.1568                      | 1.1664    | 1.2643   |
| 14 | 35            | 3                 | 625              | 175                         | 1.5981                      | 1.5441    | 1.7341   |
| 15 | 35            | 3                 | 750              | 75                          | 1.3634                      | 1.3536    | 1.4865   |
| 16 | 35            | 4.5               | 500              | 175                         | 1.7853                      | 1.9331    | 1.9781   |
| 17 | 35            | 4.5               | 625              | 125                         | 1.2559                      | 1.3574    | 1.4971   |
| 18 | 35            | 4.5               | 750              | 75                          | 1.1726                      | 1.1553    | 1.2458   |
| 19 | 45            | 1.5               | 500              | 175                         | 1.2889                      | 1.2997    | 1.3556   |
| 20 | 45            | 1.5               | 625              | 125                         | 1.2999                      | 1.4659    | 1.5567   |
| 21 | 45            | 1.5               | 750              | 75                          | 1.2634                      | 1.3568    | 1.3556   |
| 22 | 45            | 3                 | 500              | 125                         | 1.9554                      | 2.0545    | 2.1878   |
| 23 | 45            | 3                 | 625              | 175                         | 1.4521                      | 1.5698    | 1.6989   |
| 24 | 45            | 3                 | 750              | 75                          | 1.1296                      | 1.2874    | 1.3656   |
| 25 | 45            | 4.5               | 500              | 175                         | 1.4338                      | 1.5878    | 1.6598   |
| 26 | 45            | 4.5               | 625              | 125                         | 1.363                       | 1.4667    | 1.5968   |
| 27 | 45            | 4.5               | 750              | 75                          | 1.5991                      | 1.6778    | 1.7678   |

Wear resistance and hardness (74.3 HN) of sample A2 are significantly improved by 5% TiB<sub>2</sub> reinforcement and 5% nanographite reinforcement. The A2 composites, on the other hand, can perform at temperatures that are far higher than those of A and A1. A preservative barrier forms when TiB<sub>2</sub> and nanographite particulate are mixed with Al 2219, making it difficult for dislocations to occur. Wear resistance is greatly enhanced by the dispersion-strengthening effect. At ambient and high temperatures, it can be sustained for long periods of time [27, 28]. To achieve a higher level of wear resistance at 175 $^{\circ}$ C, TiB<sub>2</sub> and nanographite content is a suitable substitute to the usual alloy. The matrix phase strengthening kinetics may be improved by the presence of TiB<sub>2</sub> and nanographite particulate that is based on the experimental results. The longer sliding distance resulted in an increase in wear resistance. Thermal stresses and pressure compaction cause tearing of oxide layers during high-temperature sliding, resulting in agglomerated clusters of

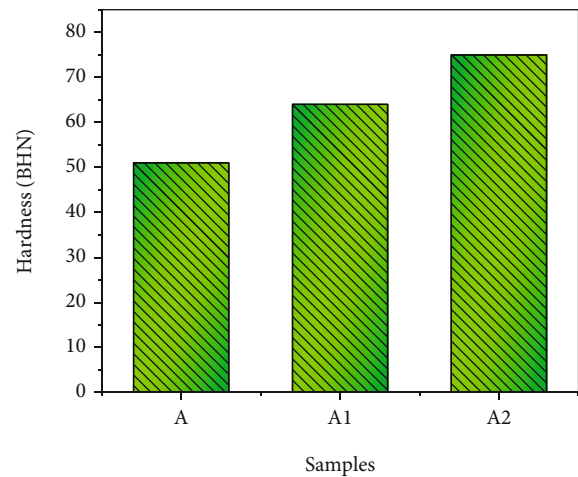


FIGURE 2: Hardness measurement for AMMC casting.

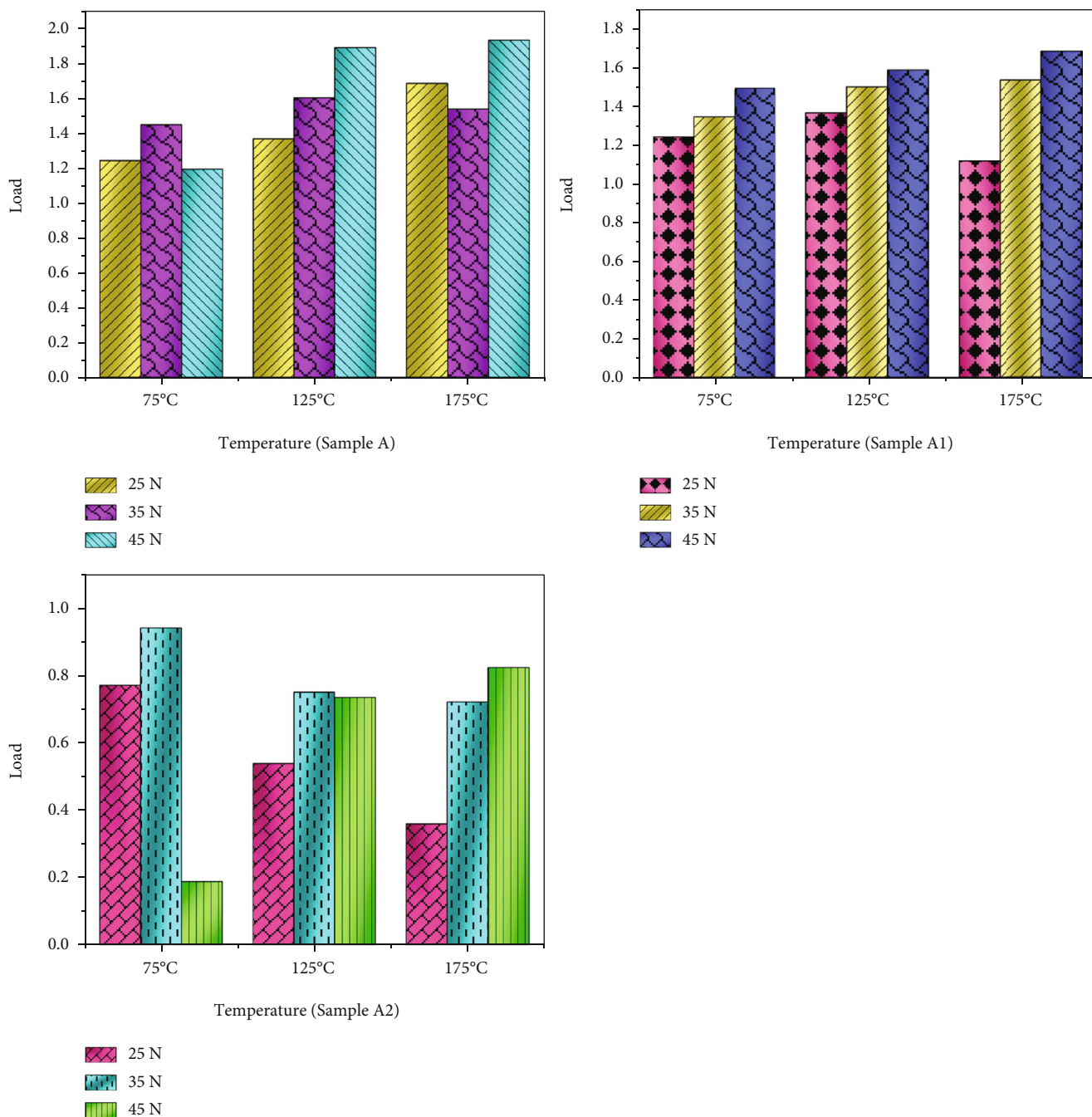


FIGURE 3: Load vs. temperature.

oxide wear debris. Due to temperature and applied pressure, fine wear debris sinters [29]. As the temperature rises, the sintering rate increases, resulting in tribolayers, which are solid, smooth, hard surfaces. The wear rate is reduced because the tribolayers protect the sliding surfaces for a longer period of time from developed forces. Wear debris is fused together after tribofailure, which results in an oxide layer being formed and torn. This process is repeated over and over again. At room temperature, the tribolayer effect on alloys and composites was unaffected,

as evidenced by the wear trend [30]. Only a few studies have examined the effect of ceramics on aluminum. In contrast to Al2219/Si<sub>3</sub>N<sub>4</sub>/nano-Gr and the unreinforced matrix, Al2219/TiB<sub>2</sub>/nano-Gr composites maintain their high-temperature strength as in Figure 4. Therefore, increasing the weight percent of TiB<sub>2</sub> and nanographite particulates, as well as the addition of this segment, is an attractive option that should be pursued [31]. Figures 5–7 show the experimental and predicted, normalized factor importance, and error values.



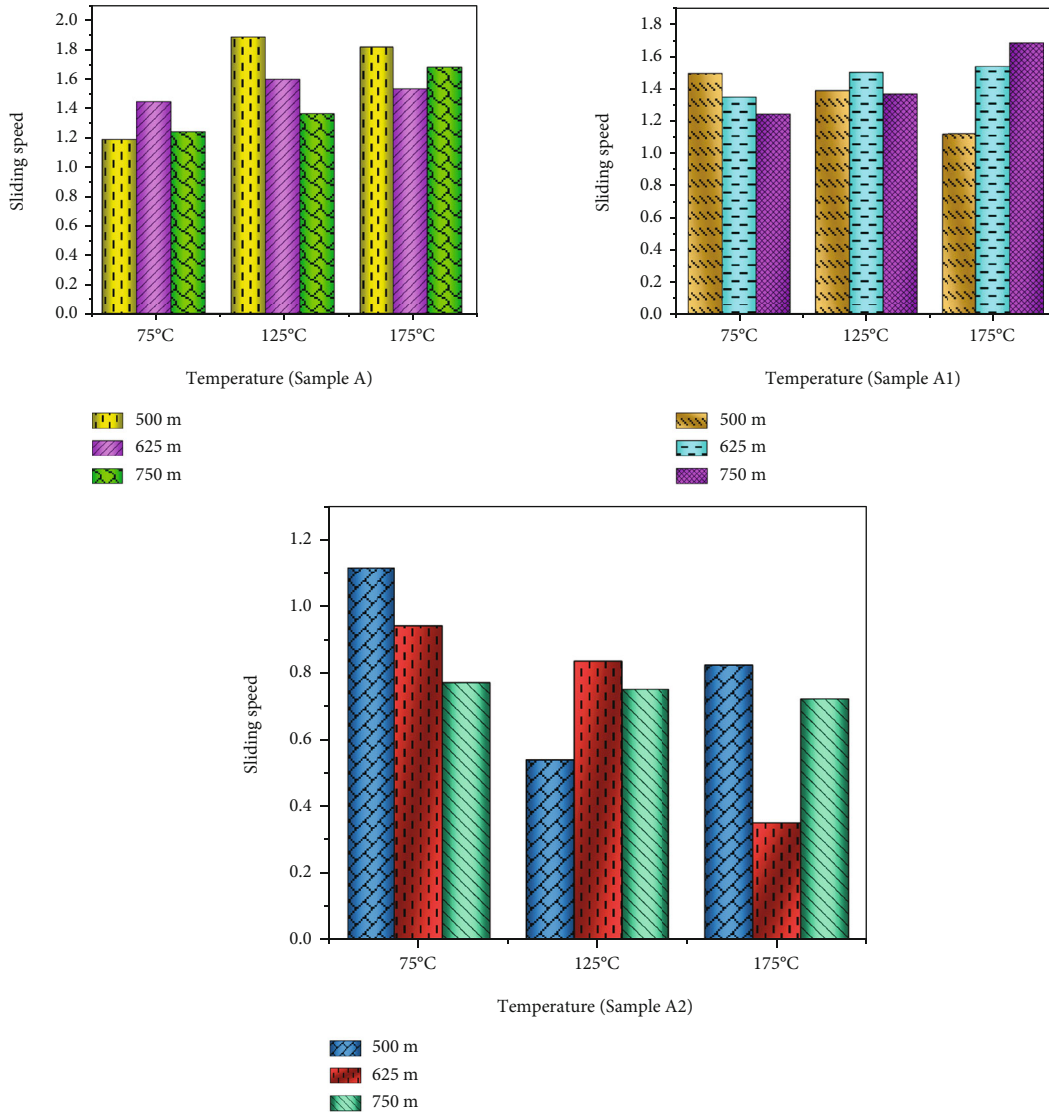


FIGURE 4: Temperature vs. sliding speed.

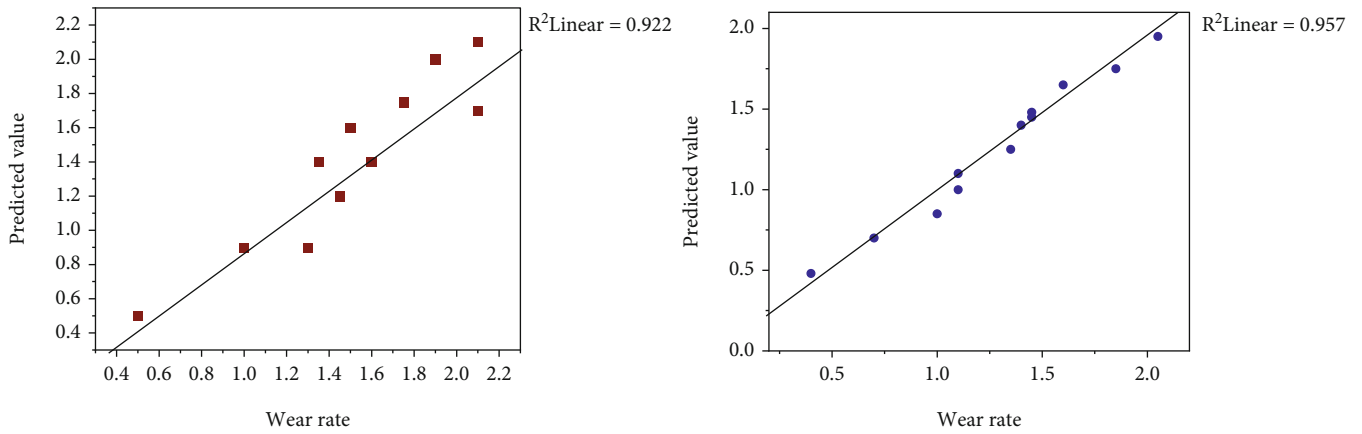


FIGURE 5: Experimental vs. predicted values.

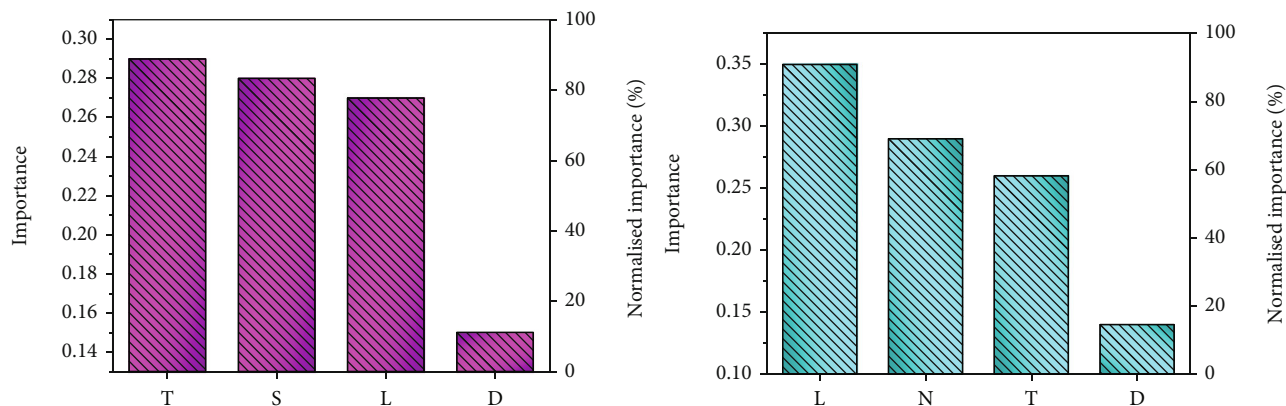


FIGURE 6: Normalized factor importance.

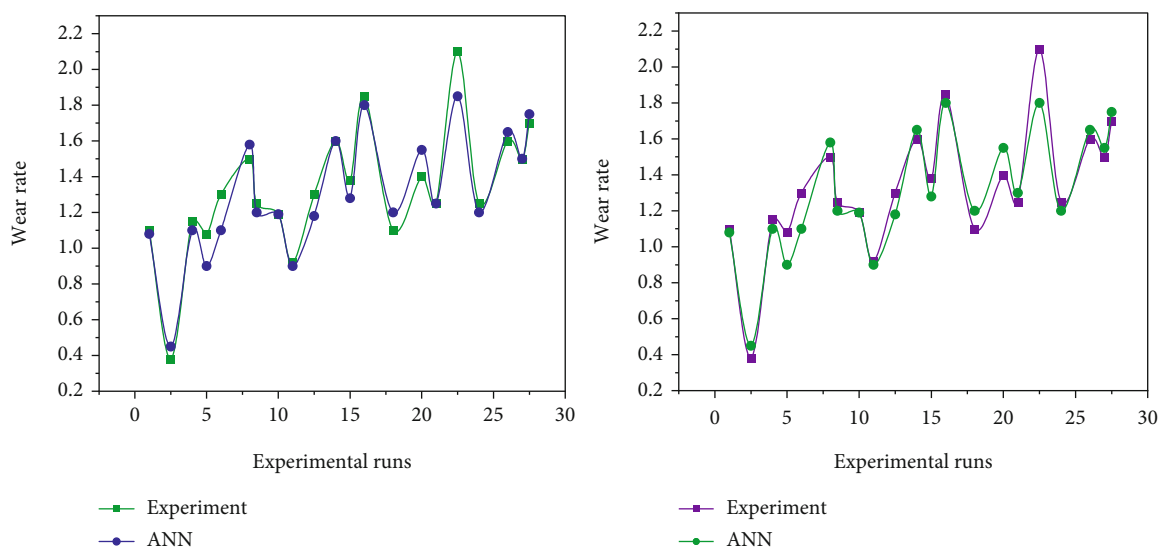


FIGURE 7: Error values.

## 4. Conclusions

Stir casting is used to create Al2219, Al2219+ Si<sub>3</sub>N<sub>4</sub> + nano-Gr, and Al2219+ TiB<sub>2</sub> + nano-Gr composites in this study. Using the L27 orthogonal array as a platform, experiments are carried out. It is possible to arrive at the following conclusions.

Consequently, it is concluded that the AMMC liquid stir casting method is preferable because it ensures proper alloy mixing.

- (i) In all temperatures, increasing the applied load and speed increases the wear rate
- (ii) The wear rate of the AMMC tribolayers was significantly influenced. In terms of wear, the titanium diboride and nanographite reinforced AMMCs (A2) have the lowest rates, while the Al2219 samples (A) have the highest rates
- (iii) Sliding is also known to cause abrasive and adhesive wear. The results showed that Al2219 metal matrix

composites could be replaced by those containing TiB<sub>2</sub> and graphite

- (iv) At 175 degrees Celsius, the hybrid composite A2 outperforms A1 and A2 in terms of wear resistance. Tribolayers formed by graphite and titanium dioxide have low deterioration rates because the tribolayer is solid. As a result, titanium diboride and nanographite-reinforced AMMCs (A2) exhibit exceptional wear resistance across a wide range of temperatures

## Data Availability

The data used to support the findings of this study are included within the article. Further data or information is available from the corresponding author upon request.

## Conflicts of Interest

The authors declare that there is no conflict of interest regarding the publication of this article.

## Acknowledgments

The authors appreciate the supports from Mizan Tepi University, Ethiopia for the research and preparation of the manuscript. The author thankfully acknowledge the funding provided by Scientific Research Deanship, King Khalid University, Abha, Kingdom of Saudi Arabia, under the grant number R.G.P.1/267/43.

## References

- [1] P. R. S. Kumar, S. Kumaran, T. Srinivasa Rao, and S. Natarajan, "High temperature sliding wear behavior of press-extruded AA6061/fly ash composite," *Elsevier -Material Science and Engineering:A*, vol. 527, no. 6, pp. 1501–1509, 2010.
- [2] J. A. Jeffrey, S. S. Kumar, V. A. Roseline, A. L. Mary, and D. Santhosh, "Contriving and assessment of magnesium alloy composites augmented with boron carbide VIA liquid metallurgy route," *Materials Science Forum*, vol. 1048, pp. 3–8, 2022.
- [3] A. Abou Gharam, M. J. Lukitsch, M. P. Balogh, and A. T. Alpas, "High temperature tribological behaviour of carbon based (B4C and DLC) coatings in sliding contact with aluminum," *Thin Solid Films*, vol. 519, no. 5, pp. 1611–1617, 2010.
- [4] V. Mohanavel, S. Prasath, K. Yoganandam, B. G. Tesemma, and S. S. Kumar, "Optimization of wear parameters of aluminium composites (AA7150/10 wt%WC) employing Taguchi approach," *Materials Today: Proceedings*, vol. 33, pp. 4742–4745, 2020.
- [5] S. M. Abarghouie and S. S. Reihani, "Investigation of friction and wear behaviors of 2024 Al and 2024 Al/SiCp composite at elevated temperatures," *Journal of Alloys and compounds*, vol. 501, no. 2, pp. 326–332, 2010.
- [6] M. Ravichandran, V. Mohanavel, T. Sathish, P. Ganeshan, S. Suresh Kumar, and R. Subbiah, "Mechanical properties of AlN and molybdenum disulfide reinforced aluminium alloy matrix composites," *Journal of Physics: Conference Series*, vol. 2027, p. 012010, 2021.
- [7] M. L. Bharathi, S. A. Rag, L. Chitra et al., "Investigation on wear characteristics of AZ91D/nanoalumina composites," *Journal of Nanomaterials*, vol. 2022, 2022.
- [8] T. Gómez-del Río, A. Rico, M. A. Garrido, P. Poza, and J. Rodríguez, "Temperature and velocity transitions in dry sliding wear of Al-Li/SiC composites," *Wear*, vol. 268, no. 5-6, pp. 700–707, 2010.
- [9] J. A. Jeffrey, S. S. Kumar, P. Hariharan, M. Kamesh, and A. M. Raj, "Production and assessment of AZ91 reinforced with nano SiC through stir casting process," *Materials Science Forum*, vol. 1048, pp. 9–14, 2022.
- [10] J. Llorca, "High temperature fatigue of discontinuously-reinforced metal-matrix composites," *International Journal of Fatigue*, vol. 24, no. 2-4, pp. 233–240, 2002.
- [11] S. Suresha and B. K. Sridhara, "Wear characteristics of hybrid aluminium matrix composites reinforced with graphite and silicon carbide particulates," *Composites Science and Technology*, vol. 70, no. 11, pp. 1652–1659, 2010.
- [12] N. Radhika, R. Subramanian, and S. V. Prasat, "Tribological behaviour of aluminium/alumina/graphite hybrid metal matrix composite using Taguchi's techniques," *Journal of minerals and materials characterization and engineering*, vol. 10, no. 5, p. 427, 2011.
- [13] A. Kumar, S. Lal, and S. Kumar, "Fabrication and characterization of A359/Al2O3 metal matrix composite using electromagnetic stir casting method," *Journal of Materials Research and Technology*, vol. 2, no. 3, pp. 250–254, 2013.
- [14] V. Auradi, G. L. Rajesh, and S. A. Kori, "Processing of B<sub>4</sub>C particulate reinforced 6061aluminum matrix composites by melt stirring involving two-step addition," *Procedia Materials Science*, vol. 6, pp. 1068–1076, 2014.
- [15] A. Ahmed, M. S. Wahab, A. A. Raus, K. Kamarudin, Q. Bakhsh, and D. Ali, "Mechanical properties, material and design of the automobile piston: an ample review," *Indian Journal of Science and Technology*, vol. 9, no. 36, pp. 1–7, 2016.
- [16] G. Rajaram, S. Kumaran, and T. S. Rao, "High temperature tensile and wear behaviour of aluminum silicon alloy," *Materials Science and Engineering: A*, vol. 528, no. 1, pp. 247–253, 2010.
- [17] S. G. Shabestari and H. Moemeni, "Effect of copper and solidification conditions on the microstructure and mechanical properties of Al–Si–Mg alloys," *Journal of Materials Processing Technology*, vol. 153, pp. 193–198, 2004.
- [18] J. R. Davis, *Corrosion of Aluminum and Aluminum Alloys*, Ohio, ASM International, 1999.
- [19] L. F. Mondolfo, *Aluminum Alloys: Structure and Properties*, Butterworths, London, 1999.
- [20] F. Gul and M. Acilar, "Effect of the reinforcement volume fraction on the dry sliding wear behaviour of Al-10Si/SiC<sub>p</sub> composites produced by vacuum infiltration technique," *Composites Science and Technology*, vol. 64, no. 13-14, pp. 1959–1970, 2004.
- [21] B. N. Sharath, K. S. Madhu, and C. V. Venkatesh, "Experimental study on dry sliding wear behaviour of Al-B<sub>4</sub>C-Gr metal matrix composite at different temperatures," *Journal of the Mechanical Behavior of Materials*, vol. 895, pp. 96–101, 2019.
- [22] H. Czichos, S. Becker, and J. Lexow, "Multilaboratory tribotesting: results from the versailles advanced materials and standards programme on wear test methods," *Wear*, vol. 114, no. 1, pp. 109–130, 1987.
- [23] "Manual on quality control of materials, ASTM STP 15D," *ASTM*, vol. 15D, pp. 1–136, 1951.
- [24] G. Singh and S. Goyal, "Microstructure and mechanical behavior of AA6082-T6/SiC/B4C-based aluminum hybrid composites," *Particulate Science and Technology*, vol. 36, no. 2, pp. 154–161, 2018.
- [25] Y. Q. Wang and J. I. Song, "Temperature effects on the dry sliding wear of Al<sub>2</sub>O<sub>3</sub>f/SiCp/Al MMCs with different fiber orientations and hybrid ratios," *Wear*, vol. 270, no. 7-8, pp. 499–505, 2011.
- [26] A. Mazahery, H. Abdizadeh, and H. R. Baharvandi, "Development of high-performance A356/nano-Al<sub>2</sub>O<sub>3</sub> composites," *Materials Science and Engineering: A*, vol. 518, no. 1-2, pp. 61–64, 2009.
- [27] R. Kaibyshev, O. Sitdikov, I. Mazurina, and D. R. Lesuer, "Deformation behavior of a 2219 Al alloy," *Materials Science and Engineering: A*, vol. 334, no. 1-2, pp. 104–113, 2002.
- [28] S. Biswas, E. Dwarakadasa, and S. K. Biswas, "Bearings and wear properties of cast graphite aluminium composites," *Proceedings of All India Seminar on Aluminium*, pp. 189–196, 1979.
- [29] G. Straffellini, M. Pellizzari, and A. Molinari, "Influence of load and temperature on the dry sliding behaviour of Al-based



- metal-matrix-composites against friction material,” *Wear*, vol. 256, no. 7-8, pp. 754–763, 2004.
- [30] H. Zhu, C. Jia, J. Li et al., “Microstructure and high temperature wear of the aluminum matrix composites fabricated by reaction from Al–ZrO<sub>2</sub>–B elemental powders,” *Powder technology*, vol. 217, pp. 401–408, 2012.
- [31] Y. X. Jin, X. Y. Wang, Q. Q. Tong, H. M. Chen, and J. M. Lee, “High-temperature Dry Sliding Friction and Wear Characteristics of As-cast SiCP/A356 Composite,” *Advanced Materials Research*, vol. 690-693, pp. 318–322, 2013.